INFLUENCE OF OXIDATION AND EMISSIVITY FOR METALLIC ALLOYS SPACE DEBRIS DURING THEIR ATMOSPHERIC ENTRY

L. Barka [(1)], M. Balat-Pichelin [(1)], J.L. Sans [(1)], J. Annaloro [(2),] P. Omaly [(2)]

[(1)] PROMES-CNRS laboratory, 7 rue du four solaire, 66120 Font-Romeu Odeillo, France
marianne.balat@promes.cnrs.fr

[(2)] CNES, 18 avenue Edouard Belin, 31401 Toulouse cedex 9, France
julien.annaloro@cnes.fr

ABSTRACT

In order to mitigate debris in orbit and to avoid dramatic collisions on Earth after atmospheric re-entry at their end-of-life, the spacecraft missions have to take into account the influence of atmospheric re-entry conditions on the spacecraft survivability.
The non-equilibrium air plasma flow impinging the material enhances oxidation phenomena and also heat flux by species recombination. Oxidation, ablation, and melting coupled phenomena can occur on the material leading to an important increase of heating and damage of the materials. In this way, oxidation in air plasma conditions close to those encountered during re-entry was studied on metallic alloys such as SS 316L and Invar in order to obtain degradation kinetic laws at high temperature (up to the melting point of the alloys) and for short time duration (few minutes).
Then, measurements of the total directional emissivity – and hemispherical values obtained by integration – at high temperature were carried out on the same virgin alloys – in secondary vacuum to avoid oxidation – and on samples pre-oxidized in air plasma conditions, and also oxidized in situ in standard air. An increase of the total emissivity for oxidized samples by a factor 3 to 4 is obtained compared to virgin samples. Some results on oxidation and emissivity obtained for SS 316L and Invar with microstructural characterization on virgin and pre-oxidized surfaces using different techniques such as SEM, XRD and 3D roughness profilometry will be presented.

1 INTRODUCTION

Nowadays, there is no international regulation for space debris. Several space actors have their own rules to limit the debris production and to better manage the explosion and collision risks on space orbits or on Earth at landing. The French space act, (LOS, Loi relative aux Opérations Spatiales) was approved by the French parliament and is applicable since December 2010. Its main objective is the security of space operations and implies that all French space operations must be subjected to prior authorization delivered by CNES. The atmospheric re-entry of spacecraft represents a very critical phase with the severe encountered aerothermodynamics and aero-thermochemical conditions. Indeed, integrity, shape and trajectory of debris from spacecraft are significantly altered. This is why, the knowledge of the materials properties obtained in atmospheric re-entry conditions becomes mandatory for the survivability modelling of the spacecraft and finally to obtain the launch authorization. To study and to assess the debris survival risks during the atmospheric re-entry, CNES has developed its own engineering tool, DEBRISK [1,2]. It allows calculating the 3D trajectory of the satellite components, the surface heat flux and the debris disappearance altitudes during the re-entry phase. However, databases currently available in DEBRISK are limited for oxidation kinetics law and for thermal radiative properties (emissivity) of materials at high temperature, parameters needed for the calculation of the final mass reaching the ground.
To increase the calculation accuracy of the DEBRISK tool, CNES collaborates with PROMES-CNRS laboratory to perform oxidation in atmospheric re-entry condition and to measure emissivity at high temperature. These new data will be implemented in the DEBRISK code.
In the literature, there are few studies on oxidation of SS 316L and Invar. Oxidation tests were mainly performed in standard air [3-6] and a little realized in air plasma or CO_2 conditions [7,8] at lower temperature than the ones we are interesting in. No emissivity data can be found in the literature for both materials. This is why oxidation in air plasma conditions and emissivity measurements at high temperature were performed in order to obtain representative data.

Proc. 7th European Conference on Space Debris, Darmstadt, Germany, 18–21 April 2017, published by the ESA Space Debris Office
Ed. T. Flohrer & F. Schmitz, (http://spacedebris2017.sdo.esoc.esa.int, June 2017)

2 EXPERIMENTAL EMISSIVITY MEASUREMENT AND DEVICE

The method developed at PROMES-CNRS laboratory for emissivity measurements is a direct one. It consists of the measurement of two parameters, the true temperature and the total or spectral directional radiance of the sample in a given wavelength range [9]. The total or spectral directional emissivity (ε) is the ratio of the measured radiance (L) of the material to the part of the blackbody radiance (L_0) at the same temperature and wavelength range according to the following relation (1) expressed as:

$$\varepsilon = L(T) / L_0(T) \qquad (1)$$

The hemispherical corresponding emissivity is calculated by integration of the directional values.
The experimental set-up MEDIASE (Moyen d'Essai et de DIagnostic en Ambiance Spatiale Extreme) shown in Fig. 1 is placed at the focus of the 1 MW Odeillo solar furnace in order to reach very high temperature in a few seconds. It allows studying the physico-chemical behavior of materials under extreme conditions at very high temperature (up to 2500 K). The set-up consists of a stainless steel vessel with a capacity of 6.10^{-2} m^3, equipped with a turbo-molecular pumping system allowing working in high vacuum conditions (up to 10^{-5} Pa). A hemispherical silica-glass window (35 cm diameter) allows the heating of the sample (40 mm diameter, 2 mm thickness) with concentrated solar radiation by the gradual opening of the doors of the solar furnace, the high vacuum being preserved inside the vessel. The true temperature of the sample is measured on the back face using a two-color pyro-reflectometer developed in our laboratory [10] and calibrated on a blackbody before and after each measurements series up to 1900 K. The directional radiance measurements are performed using the radiometer equipped with a Cassegrain optic (KT4 Heimann, Germany). According to the needed wavelength range, the radiometer is used without filter (0.6-40 μm) or with narrow spectral filters (2.7; 5 or 5.5 μm) or spectral band filters (0.6-2.8; 3-5; 7-10; 8-14 μm). Directional radiance measurements are performed with an original motorized three-mirrors system goniometer, developed in our laboratory, in such a way the sample and the radiometer stay fixed. The directional data are acquired from 0 to 60° or 80° for respectively sample diameters of 25 or 40 mm. The window placed between the sample and the radiometer is adapted for the used wavelength range. It is composed of thallium iodobromide (KRS5) in order to perform measurements from 0.6 to 40 μm. The whole system radiometer-optical window-goniometer is calibrated before and after each series of measurements on a blackbody as for the optical pyro-reflectometer. The uncertainty on emissivity is around 3% between 1500 and 2300 K for the spectral range of 0.6 to 40 μm.

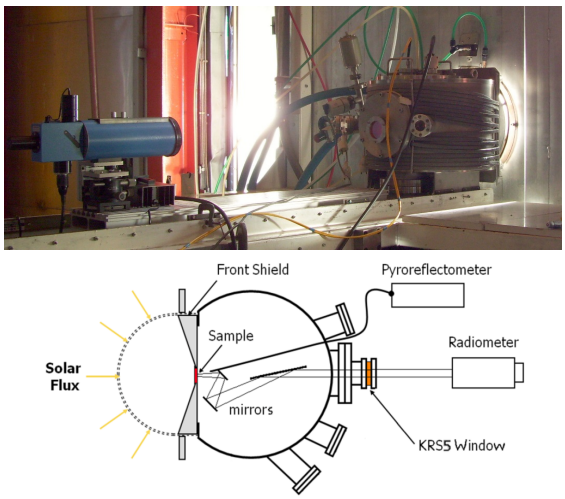

Figure 1. Picture and scheme of the MEDIASE device in the emissivity measurement configuration

3 OXIDATION IN AIR PLASMA CONDITIONS

The experimental set-up MESOX (Moyen d'Essai Solaire d'OXydation) shown in Fig. 2 is placed at the focus of the 6 kW solar furnace equipped with a variable opening shutter. It allows simulating on Earth the encountered conditions during the atmospheric re-entry (air plasma, high temperature and low pressure) of materials [11]. The set-up MESOX is equipped with a microwave generator (2450 MHz, 1200 W max) and a waveguide for creating non-equilibrium air plasma. A regulator, a gauge and a vacuum pump allow controlling precisely the total air pressure during the experiment. The incident concentrated solar flux can reach 5 $MW.m^{-2}$. The temperature measurement is performed on the front face of the sample by using a monochromatic (5 μm) optical pyrometer with a system of two mirrors. In this study, air plasma is created by a 300 W discharge surrounding the sample (15x15x2 mm^3 for oxidation studies and 25 mm diameter, 2 mm thickness for emissivity measurement) and the total air pressures are fixed at 300 and 2000 Pa. The air flow is set at 4 l/h to obtain a maximum oxygen dissociation rate of 80 % [12]. The mass variation of the sample before and after test was measured to monitor the influence of the oxidation on the material. Microstructural characterizations were also carried out by different techniques such as SEM, 3D roughness profilometry and XRD before and after oxidation to know the morphology and the

composition of the oxide layer formed on the sample surface.

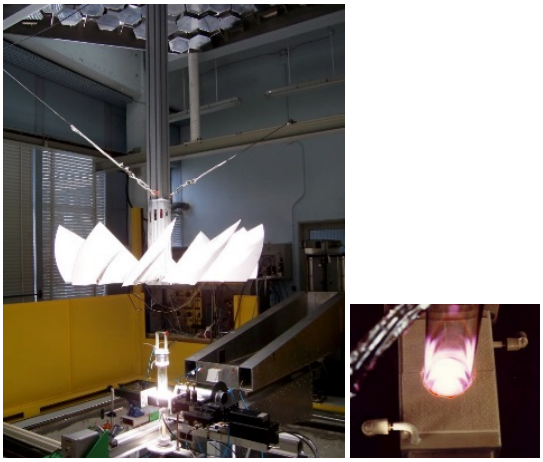

Figure 2. Pictures of the MESOX device (on the left) and air plasma (on the right)

4 EXPERIMENTAL RESULTS

In this section, the metallic alloys selected and the experimental results obtained for the study of the oxidation in air plasma conditions and for the emissivity are reported and discussed.

4.1 Materials

The materials used in this study are metallic alloys such as SS 316L and Invar provided by Goodfellow. The compositions of each material are the following for the main components:
- SS 316L: Fe 70%; Cr 17%; Ni 10 %; Mo 2% and Mn 1%
- Invar: Fe 64% and Ni 36%.

4.2 Emissivity in high vacuum

In order to know the thermal radiative properties of virgin SS 316L samples, total directional emissivity measurements and total hemispherical emissivity calculation - obtained by integration of the directional values - were performed in high vacuum (10^{-4} Pa). Emissivity of materials is dependent on the wavelength, the angle of emission and also the surface morphology (rough or smooth). In this way, total directional emissivity measurements were performed on rough (sand-blasted) and smooth (as-received) SS 316L samples for several temperature levels in the total wavelength range (0.6-40 μm) from 0° to 80° incidence angle as the samples are 40 mm in diameter. Fig. 3 reports the evolution of the total directional emissivity of a smooth SS 316L sample for several temperatures. It can be observed the decrease of the emissivity with the temperature increasing from 1101 K to 1384 K and also, the increase of the emissivity for higher angles characteristics of metallic materials.

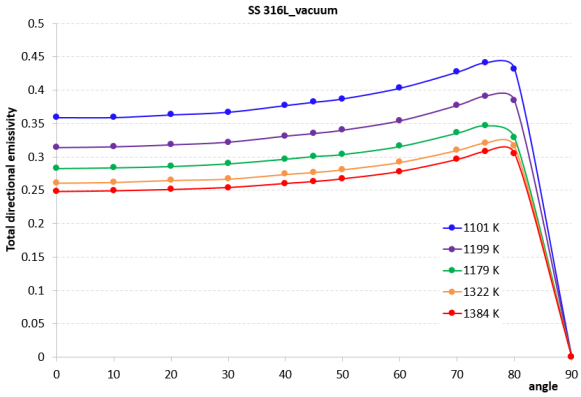

Figure 3. Total directional emissivity versus angle of emission for a smooth SS 316L sample in high vacuum for several temperatures.

Scanning Electron Microscopy (SEM) was performed on the samples before and after emissivity measurement. SEM images for - smooth and rough - SS 316L samples before and after emissivity measurement in high vacuum and temperature conditions are presented in Figs. 4 and 5. For both surfaces, it can be observed, after reaching the highest temperature level, a growing of the grains, feature of the smoothing of the surface.

Smooth SS 316L (T_{max} = 1373 K)

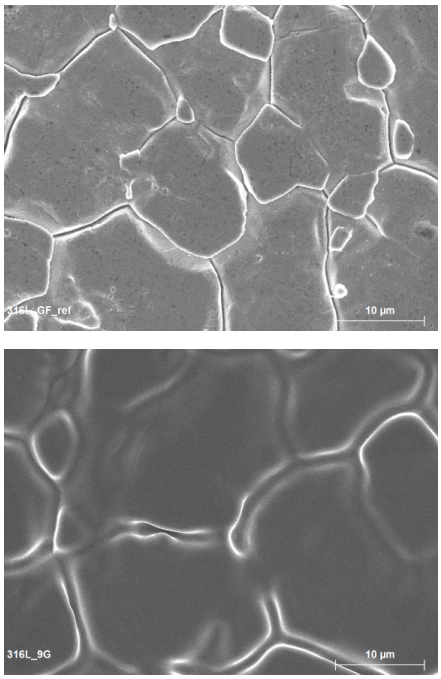

Figure 4. SEM images for smooth SS 316L surface samples before (top) and after (down) emissivity measurements in high vacuum at around 1373 K. The scale bar is 10 µm

Rough SS 316L (T_{max} = 1375 K)

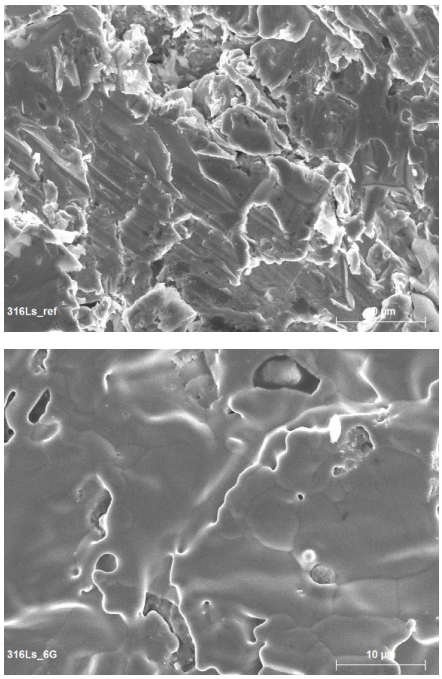

Figure 5. SEM images for rough SS 316L surface samples before (top) and after (down) emissivity measurements in high vacuum at around 1375 K. The scale bar is 10 µm

The evolution of the total hemispherical emissivity for smooth (round marker) and rough (square open marker) SS 316L samples in high vacuum versus temperature is reported in Fig. 6. Regardless of the surface morphology, the total hemispherical emissivity of SS 316L samples decreases in the temperature range 1100-1300 K and become nearly constant - around 0.25-0.30 - in the high temperature range up to 1450 K.
Nevertheless, the effect of the surface roughness is mainly visible for the lower temperature range. Table 1 reports the values of the roughness parameters for the samples before and after emissivity measurement: Sa is the arithmetic value and Sq the mean square surface roughness.

Table 1. Roughness parameters for SS 316L samples before and after emissivity measurement at high temperature

Sample Roughness parameters	Smooth before ε	Smooth after ε	Rough before ε	Rough after ε
Sa (µm)	0.11	0.01	0.40	0.36
Sq (µm)	0.24	0.17	0.57	0.48

The differences that can be observed for the emissivity values in the lower temperature range are clearly related to the surface morphology as reported in Table 1. After the smoothing of the sample surface due to the grain grow at high temperature, this difference is suppressed as it can be seen in Fig. 6.

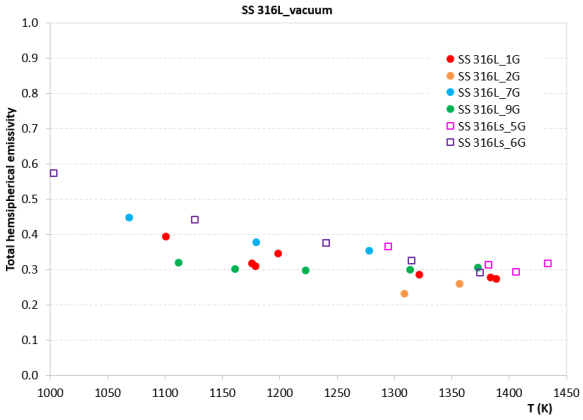

Figure 6. Evolution of the total hemispherical emissivity versus temperature for - smooth and rough - SS 316L samples

4.3 Oxidation in air plasma conditions

Invar and SS 316L samples were oxidized in air plasma conditions in the MESOX set-up under 300 or 2000 Pa for duration around 360 s. The mass variation, expressed in g/m^2.s, after oxidation at 300 Pa versus temperature for both materials is reported in Fig. 7. The mass gain for Invar is clearly huge than that of the SS 316L in the same temperature range.

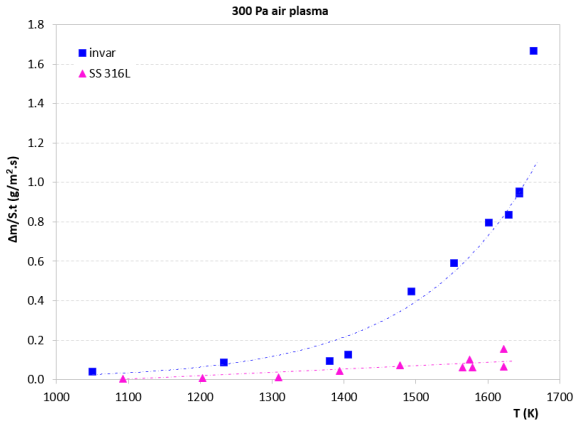

Figure 7. Mass variation versus temperature for Invar and SS 316L samples oxidized in air plasma at 300 Pa

The significant difference of the mass gain for both materials at around 1500 K and 300 Pa for an oxidation duration of 300 s is reported in Table 2.

Table 2. Mass gain value (in g/m^2) for SS 316L and Invar samples at around 1500 K

SS 316L	10
Invar	134

X-Ray Diffraction (XRD) analyses presented in Fig. 8 were performed after oxidation in air plasma conditions at 300 Pa for SS 316L and Invar and are compared with the reference material (before oxidation). The XRD patterns present the peaks corresponding to the same iron oxides (Fe_2O_3 and Fe_3O_4) but with different crystalline orientations. For the lowest oxidation temperature, the formation of mainly Fe_2O_3 oxide (hematite structure) is observed for both materials. However, when the temperature increases, a clearly reduction of the Fe_2O_3 peaks for both materials is observed and an important increase of the Fe_3O_4 (magnetite structure) peak at $2\theta = 44°$ for Invar sample can be seen.

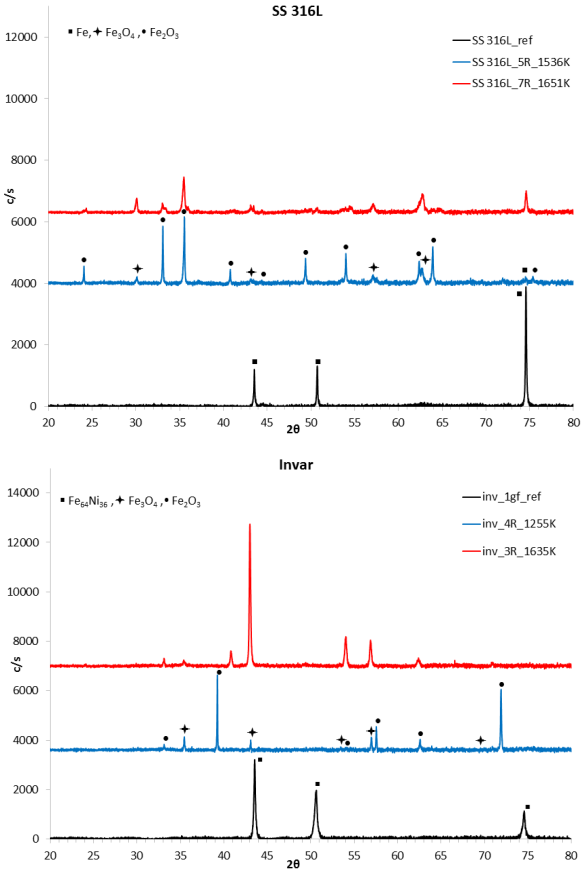

Figure 8. XRD patterns of some SS 316L and Invar samples showing the presence of crystallized oxides compared to the reference

Fig. 9 presents the picture of the surfaces of oxidized Invar samples (on the left) and the corresponding SEM image (on the right) at two temperatures 1255 K and 1635 K. These pictures show the color change of the oxide layer with the temperature increasing. For the lowest temperature 1255 K, the oxide layer is brown and turns to gray at 1635 K. Furthermore, it can be noticed in the SEM images, the significant surface smoothing with the temperature increasing. The mean surface square roughness Sq values are equal to 1.40 µm (1255 K) and 0.12 µm (1635 K) assessing the decrease of the surface roughness with the temperature increase.

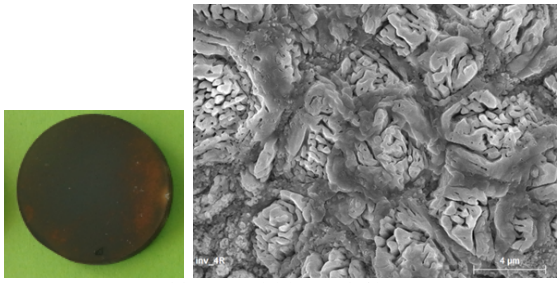

1255 K, 300 Pa, 360 s

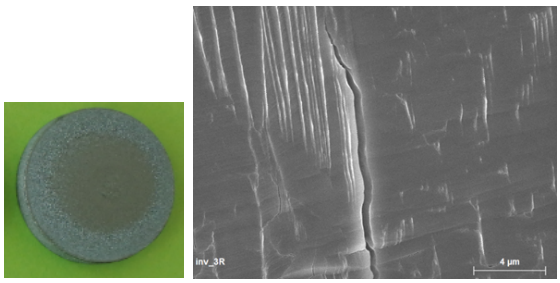

1635 K, 300 Pa, 360 s

Figure 9. Pictures (on the left) and SEM images (on the right) of oxidized Invar surfaces. The scale bar is 4 µm

4.4 Emissivity on pre-oxidized materials

Measurements of the total normal emissivity were performed on SS 316L pre-oxidized samples at 300, 500 or 2000 Pa in air plasma conditions in the MESOX set-up: SS 316L_7R (1650 K, 300 Pa), SS 316L_3R (1720 K, 500 Pa), SS 316L_2R (1525 K, 2000 Pa), SS 316L_8R (1645 K, 2000 Pa) and SS 316L_9R (1670 K, 2000 Pa) from about 1000 to 1750 K depending on the materials. The total normal emissivity is only reported in Fig. 10 - as the sample diameter is 25 mm - versus temperature for pre-oxidized surfaces but also for virgin surfaces (SS 316L_1G, 9G and 7G) in order to show the influence of the oxidation on the emissivity.

The global increase of the total normal emissivity with temperature is observed for the pre-oxidized samples. Furthermore, an emissivity value around 0.90 in the temperature range 1350-1750 K due to the presence of oxides can be noticed, three times higher than the emissivity values obtained for the virgin (as-received) samples.

Consequently, the knowledge of the total normal emissivity for the SS 316L pre-oxidized in air plasma conditions is mandatory to model the debris survivability and more particularly, to calculate the surface heat flux and the mass reaching the ground after the atmospheric re-entry phase.

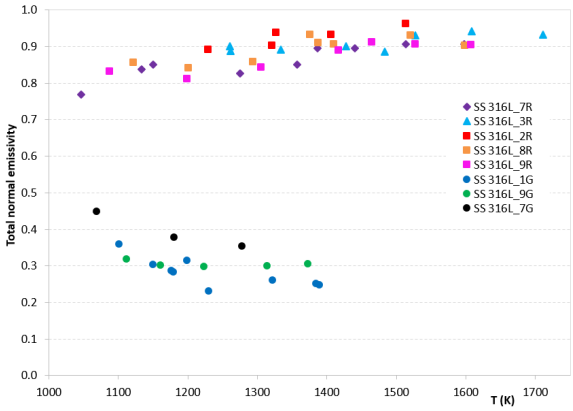

Figure 10. Total normal (0.6-40 µm) emissivity versus temperature for SS 316L virgin (as-received) and pre-oxidized in air plasma conditions

XRD analyses presented in Fig. 11 are performed on pre-oxidized SS 316L samples before and after emissivity measurement at 2000 Pa. Before emissivity measurement, the oxide layer was only composed of iron oxides such as Fe_2O_3 and Fe_3O_4. After emissivity measurement, the same oxides were identified. Furthermore, it can be observed a weakly - increase of the Fe_3O_4 and decrease of the Fe_2O_4 - oxide peaks after emissivity measurement.

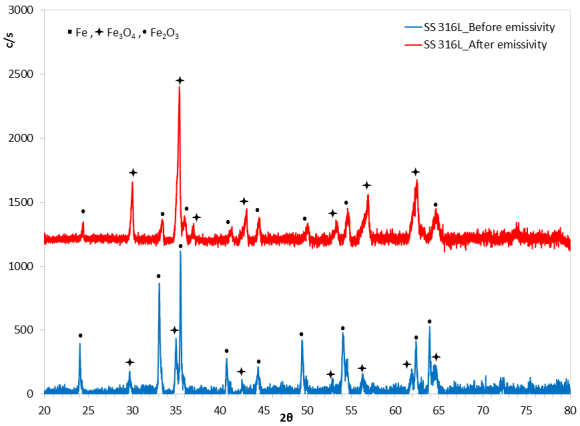

Figure 11. XRD patterns of pre-oxidized SS 316L samples (before emissivity) and after emissivity measurement

SEM images of the SS 316L samples before and after emissivity measurement at high temperature and the 3D corresponding surface roughness images are respectively presented in Figs. 12 and 13. Before emissivity measurement, a heterogeneous surface with like-flower oxides in some locations can be observed whereas after the emissivity measurement, the surface seems to be more homogeneous. Despite the morphology difference between before and after emissivity measurement, there is no evolution of the surface roughness. Indeed, the mean surface square roughness Sq measured are equal to 1.97 µm (before) and 1.80 µm (after).

Before emissivity measurement (pre-oxidized at 1642 K, 2000Pa)

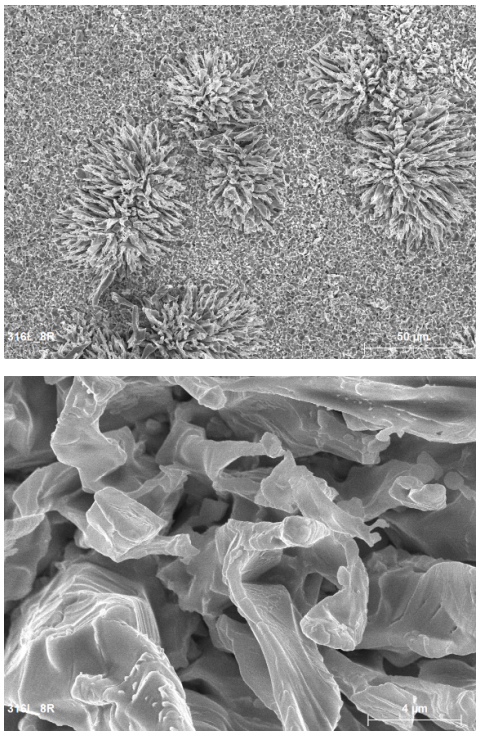

After emissivity measurement (pre-oxidized at 1705K, 2000 Pa)

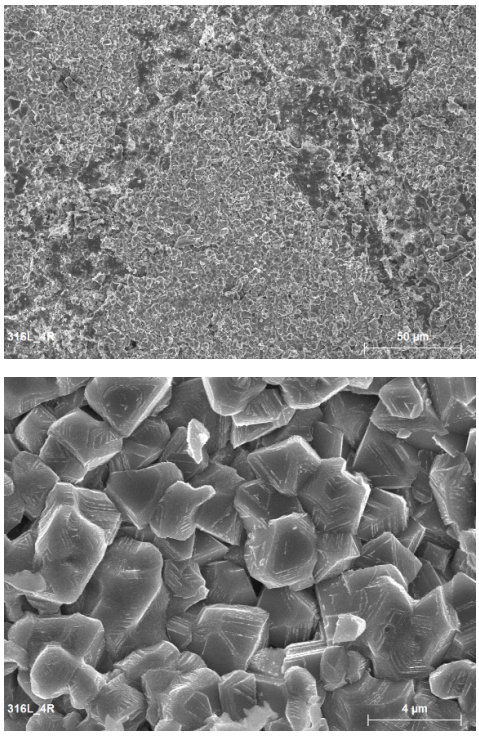

Figure 12. SEM images of the surfaces of SS 316L pre-oxidized samples before and after emissivity measurement at the same temperature level. The bar scale is 50 µm (top) and 4 µm (down)

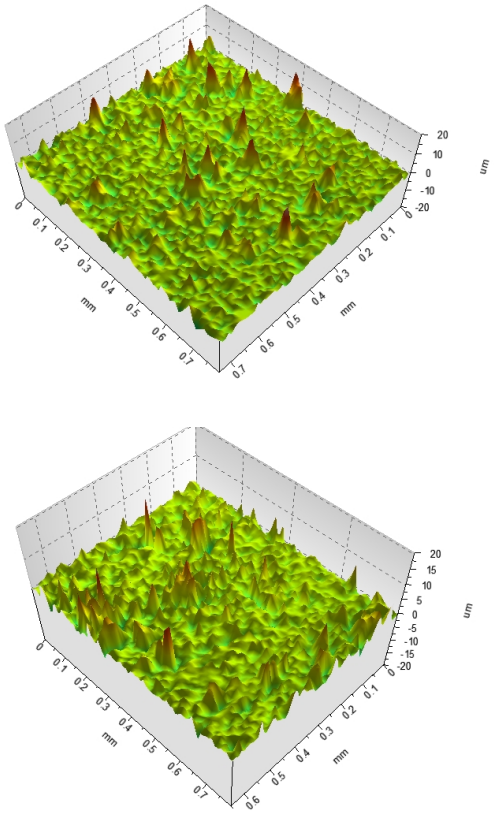

Figure 13. 3D surface roughness images of the SS 316L pre-oxidized samples before and after emissivity measurement at the same temperature

5 CONCLUSION

SS 316L and Invar alloys were oxidized in air plasma conditions at high temperature and low pressure in order to study their behavior during the atmospheric re-entry on Earth. When increasing the temperature, both materials gain mass even if the mass gain is clearly huge for Invar by more than one order of magnitude. The oxides formed in these conditions are mainly Fe_2O_3 and Fe_3O_4 for both materials with a predominant presence of magnetite at high temperature for Invar.
Emissivity measurements were also performed on SS 316L virgin surfaces in high vacuum and on pre-oxidized surfaces in air plasma conditions. A significant increase of the total normal emissivity by a factor 3 is obtained for pre-oxidized samples compared to virgin ones. So, it clearly appears that emissivity values obtained on pre-oxidized samples are mandatory for the implementation in the DEBRISK tool to better model the mass reaching the ground.

ACKNOWLEDGMENTS

This work was partly supported by the Programme “Investissements d’Avenir” (Investment for the Future) of the Agence Nationale de la Recherche (National Agency for Research) of the French State under awards numbers ANR-10-LABX-22-01-SOLSTICE through the funding of the PhD position of L. Barka and ANR-10-EQPX-49-SOCRATE.

REFERENCES

1. Omaly P., Spel M. (2012). DEBRISK, a tool for re-entry risk analysis, *Proc. 5th IAASS Conf. ‘A Safer Space for a Safer World’*, Versailles (Fr), 17-19 oct. 2011, ESA SP-699.

2. Omaly P., Magnin Vella C., Galera S. (2013). DEBRISK, CNES tool for re-entry survivability prediction: validation and sensitivity analysis, *Proc. 6th IAASS Conf. ‘Safety is not an option’*, Montréal (Ca).

3. Guo X., Kusabiraki K., Saji S. (2002). High-temperature scale formation of Fe-36%Ni bicrystals in Air, *Oxid. Met*. **58**, 589-605.

4. Wang X., Wang L., Zhu M., Zhang J., Lei M. (2006). Influence of high-intensity pulsed ion beams irradiation of oxidation behaviour of 316L stainless steel at 700°C, *Trans. Non Ferrous Met. Soc*. **16**, 676-680.

5. Buscail H., El Messki S., Riffard F., Perrier S. (2008). Role of molybdenum on the AISI 316L oxidation at 900°C, *J. Mater. Sci*, **43**, 6960-6966.

6. Labrador N., Lefort P. (1999). Oxydation de l’invar sous air, *Chem. Phys*. **96**, 810-829.

7. Vessel A., Mozetic M., Drenik A., Hauptman N., Balat-Pichelin M. (2008). High temperature oxidation of stainless steel AISI316L in air plasma, *Appl. Surf. Sci*, **255**, 1759-1765.

8. Menecier S., Valette S., Denoirjean P. (2012). Invar oxidation in CO_2, kinetics and mechanism of formation of a wustite layer, *Therm. Anal Calorim*. **107**, 607-616.

9. Balat-Pichelin M., Robert J.F., Sans J.L. (2006). Emissivity measurements on carbon-carbon composites at high temperature under high vacuum, *Appl. Surf. Sci*. **253**, 778-783.

10. Hernandez D., Sans J.L., Netchaieff A., Ridoux P., Le Sant V. (2009). Experimental validation of a pyroreflectometric method to determine the true temperature on opaque surface without hampering reflections, *Measurement.* **42**, 836-843.

11. Balat-Pichelin M., Charpentier L., Panerai F., Chazot O., Helber B., Nickel K. (2015).

Passive/active oxidation transition for CMC structural materials designed for the IXV vehicle re-entry phase, *J. Eur. Ceram. Soc.* **35** (2), 487-502.

12. Balat-Pichelin M., Vesel A. (2006) Neutral oxygen atom density in the MESOX air plasma solar furnace facility, *Chem. Phys.* **327** (1), 112-118.